The effect of mixing sequence on the block copolymer compatibilization of polybutadiene-natural rubber blend

Keqiang Wang[1], Shuo Zhong[1], Jia Fu[2], Wenjin Wang[1] and Zhongren Chen[2, a]

[1]*Department of Polymer Science and Engineering, Faculty of Materials Science and Chemical Engineering, Ningbo University, Ningbo 315211, P.R. China*
[2]*Department of Chemistry, Southern University of Science and Technology, Shenzhen 518055, P.R. China*

Abstract. The remarkable effect of the mixing sequence on the block copolymer compatibilization was investigated in this study, where a liquid butadiene-isoprene copolymer rubber (LIR-390) was used to compatibilize the polybutadiene/natural rubber (BR/NR, 30/70) blend. We have found that properly chosen mixing sequence would greatly improve the effectiveness of LIR-390 compatibilization in NR/BR blend. When LIR was first mixed with NR, and then blended with BR, the NR/BR/LIR blend showed the best compatibilization, as the AFM phase morphology revealed the significantly reduced domain size of dispersed BR phases. It is unusual that both the processing characteristics of this unvulcanized blend and the mechanical properties of its vulcanizate are improved: the unvulcanized blend had the lowest G′ and η*, while the vulcanizate had the highest G′ and η* among four controls. We attribute this phenomenon to the "sliding effect" of the uncured sample and the "networking effect" of LIR with NR and BR at the interface after vulcanization. The fatigue crack propagation measurement revealed the lowest crack growth rate for M3.
Keywords: mixing sequence; block copolymer; compatibilization; rubber blend.

1 Introduction

Polymer blends consisting of two or more components provide an efficient way to fill new and unique requirements for material properties that cannot obtained from the constituent polymers alone[1-10]. However, most pairs of polymers are thermodynamically incompatible, resulting in a two or multi-phase morphology, a narrow interface, poor physical and chemical interactions across the phase boundaries, and eventually poor mechanical properties. This problem can be alleviated to some degree by the addition of certain compatibilizers[11-16], usually suitably chosen block or graft copolymers, with segments that are chemically identical to those in the respective homopolymer phases. Theoretically these polymeric surfactants should reside in the interface, not only minimizing the contacts between the unlike segments of the copolymer and homopolymer but also displacing the two homopolymers away from the interface, thereby decreasing the enthalpy of mixing between the homopolymers[17-22]. As pointed out by Paul[1], the localization of the copolymer at the interface, with the block or graft extending into their respective homopolymer phases.

Some theoretical and experimental researches have been reported on the compatibilization action of block copolymers in heterogeneous polymer blend systems. The effect of the concentration,

[a] Corresponding author : chenzr@sustc.edu.cn

© 2016. The authors – Published by Atlantis Press

molecular weight, and the relative lengths of two blocks in block copolymers on the morphologies of emulsified phases in heterogeneous polymer blends were investigated. According to references[23-33], it is found that: small minor phase drops were coated with block copolymers formed in the interface and these drops also contained block copolymer micelles in A/B/A-b-B ternary blend[23-27]; the domain size of the dispersed phase in binary blends decreased sharply with the addition of small amounts of corresponding block copolymer, followed by a levelling off as the copolymer content was continually increased[28-30]; there appeared to be an optimum value of block copolymer molecular weight concerning the block copolymer compatibilization[31]; the best compatibilizing action was obtained with the symmetric block copolymer and whose molecular weight was higher than those of the homopolymers[32-33]. In addition, several scholars examined the influence of the architecture[34-39] of compatibilizer on the ability to emulsify a polymer blend. However, their findings appear to be inconsistent. Kim *et al.*[40] even demonstrated for the first time that compatibilization of an immiscible blend can be achieved via the addition of gradient copolymer during melt processing.

Recently, a small amount of studies focused on the influence of processing conditions or reactive compatibilization[41-46] on polymer blends, but few emphasized the importance of mixing strategy in processing. Chen *et al.*[47] disclosed a method for mixing rubber compositions with desirable filler distribution or reduced domain size of the different polymers, which gives us great inspiration in the respect of block copolymer compatibilization. This work aims to investigate the effect of the mixing sequence on the block copolymer compatibilization in order to explore a processing strategy that forcedly distributing most of the block copolymer into the interface, improving the compatibilizing efficiency when added low concentrations of copolymers and saving the cost of final blend materials. A model system composed of natural rubber (NR) and high-cis butadiene rubber (BR) homopolymers has been chosen due to their end use in tires and a liquid butadiene-isoprene copolymer rubber (LIR-390, Kuraray Co.) is available as the compatibilizer. The effect of the mixing sequence between three components on the morphology and the final properties were investigated.

2 Experimental

2.1 Materials

NR (Standard Vietnamese Rubber SVR3L, Vietnam), BR (BR9000, $ML_{1+4}^{100\,^{\circ}C}$= 40-50, cis-1, 4= 96%-98%, Yueyang Petrochemical Co., China), and liquid butadiene-isoprene copolymer rubber (LIR-390, Kuraray Co, Japan) were selected as the rubber components for this study. The number-average molecular weight (M_n) and polydispersity (PDI) of BR9000 by GPC at 30 ^{o}C is 16.36×10^4 g/mol and 4.01, respectively. The molecular weight ratio of butadiene to isoprene in LIR390 is 90:10 and its' viscosity-average molecular weight is 4.8×10^4 g/mol, which were supplied by the manufacturer and proved by our experimental characterization.

2.2 Blends preparation

The blend ratio of NR/BR blends was kept constant (70/30) and LIR390 was added to NR/BR blends by 5 wt%, replacing the corresponding portions of NR and BR. The same cure system was employed for all the compounds, and was selected with grades typical for the rubber industry. For the blends with compatibilizer, three different mixing sequences (M2, M3, M4) were applied in Table 1.

All the blends studied were prepared in three-stage mixing in an internal mixer (Haake Polylab 3000) at 50 ^{o}C and 60 rpm for 10 min. NR was masticated before mixing. For the control uncompatibilized blend (M1), the blend was mixed with the same time as compatibilized blends in all three stages in order to undergo the same thermomechanical history.

From Table 1, for M2, NR and BR were mixed in stage I, and LIR was added in stage II, which is similar to the conventional one-pot mixing. For M3, LIR was first mixed with NR in stage I and then

© 2016. The authors – Published by Atlantis Press

blended with BR in stage II, while for M4, LIR was mixed with BR in stage I and NR was added in stage II. In all blends, cure systems were added in stage III.

These four samples were vulcanized to 2 *mm* thick sheets using an electrically heated press (2518, Carver, United States) at 160 ^{o}C for the optimum cure time (t_{90}), calculated from a cure meter (MD-3000A, GTECH), and the cure behaviors were recorded simultaneously with the cure meter in accordance with ASTM Standard D2084-92. For comparing the rheological and dynamic mechanical properties of unvulcanized and vulcanized samples, unvulcanized rubber samples were also prepared without the addition of the cure system in stage III.

Table 1. Mixing sequences and polymer ratios of rubber blend specimens

Steps	Composition	**M1**	**M2**	**M3**	**M4**
I	NR	70	67.5	67.5	0
	BR	30	27.5	0	27.5
	LIR	0	0	5	5
II	NR	0	0	0	67.5
	BR	0	0	27.5	0
	LIR	0	5	0	0
III	ZnO	3	3	3	3
	St-acid	2	2	2	2
	Sulfur	2.5	2.5	2.5	2.5
	CZ	1.2	1.2	1.2	1.2

2.3 Morphology studies

Thin sections of approximately 100 *nm* thick of unvulcanized samples were obtained by cryoultramicrotomy at -140 ^{o}C in liquid nitrogen atmosphere using a LEICA EM UC7 microtome with a diamond knife. The sections were then transferred onto the silicon substrates. Without staining or etching, their surfaces were straightly investigated using a commercial atomic force microscope (AFM5500, Agilent Co). AFM measurements were operated in the tapping mode under ambient conditions using silicon cantilever probe tips (PPP-NCH, Agilent) with nominal spring constant of 42 N/m and resonance frequency of -330 kHz as specified by the manufacturer. Typically phase images were collected in order to distinguish the NR and BR regions.

2.4 Rheological behaviors characterization

Both unvulcanized and vulcanized blend samples for rheological analysis were obtained by compression molding in a mold of 25-mm diameter and 2-mm thickness, respectively. The rheological measurements of four blend samples were performed using a strain-controlled rheometer (Haake Mars III) under dry nitrogen atmosphere. A parallel-plate configuration was used with a gap size of 0.9 mm and plate diameter of 25 mm. Stress sweep tests were performed for all blends to define the linear viscoelasticity region. Dynamic frequency sweep tests were performed for unvulcanized blends at a temperature of 50 ^{o}C and for vulcanized blends at 160 ^{o}C, at the frequency region of 0.01-100 Hz. The dynamic storage modulus (G′) and the complex viscosity (η^{*}) were analyzed simultaneously.

2.5 Mechanical properties test

Dumbbell-shaped specimens were cut from vulcanized rubber sheets. Tensile strength and elongation at break were measured on tensile tester (1121, Instron) at room temperature and at a crosshead speed of 500 mm/min according to the procedure described in ASTM Standard D412. Each tensile value reported was the average of 10 tests.

© 2016. The authors – Published by Atlantis Press

2.6 Dynamic mechanical properties test

Dynamic mechanical properties of compounds were measured over a wide temperature range from -120 to 70 ^{o}C using a dynamic mechanical analyzer (DMA+1000, MetraviB). Unvulcanized and vulcanized blend samples of dimensions 30×10×2 mm^3 were used for testing. The frequency and dynamic deformation were set to 10 Hz and 1 %, respectively. The measurements were performed according to the procedure described in ASTM Standard D2231.

2.7 Fatigue crack propagation measurement

Crack growth characteristics of rubbery materials are important factors determining the strength and durability of the materials. So it is necessary to define the means of measuring the fatigue crack growth rate of rubbery materials[48-50]. In this paper, the fatigue crack growth behavior under the applied dynamic stress is usually expressed as the length of crack growth per each repeating cycle (*dc/dn*) as a function of the tear energy (*T*)[51]. Testing was measured on a specimen having the specifications according to the procedure described in ASTM Standard D412. Two notches of 1 mm in depth were cut in both short edges of the specimen with a razor blade, care being taken to ensure as nearly as possible that the cut was perpendicular to the edge as well as the strain and that the tip was normal to the major surface. The fatigue crack propagation rates were determined from cyclic loading tests performed on an original real-time monitoring system of fatigue crack propagation (MetraviB, DMA+300) at ambient conditions at 10 Hz using a sinusoidal wave form. The *dc/dn* value vs. the tear energy was recorded, with a lower crack propagation speed indicating a better crack growth resistance.

3 Results and discussion

3.1 Morphology

In the past, electron microscopy has been the primary method for determining polymer morphology[52-53]. This technique provides morphological information with nanometer scale resolution. However, in this technique, sample preparation and analysis are time consuming and require a very high level of expertise such as etching or staining. Recently the Atomic Force Microscopy (AFM) has evolved rapidly into a powerful tool, and has provided a new capability for determining polymer morphology with nanometer or better resolution[54-58]. AFM operation is based on detecting the cantilever deflection which is caused by the tip-sample force interaction, due to the difference of viscoelasticity or phase shift[59]. The phase shift of cantilever oscillation varies in response to the viscoelastic properties of the sample surface, and the domain size of each componentcan be distinguished precisely. Thus, the fine morphological features of rubber blend are easily observed in phase images.

Tapping AFM phase images of unvulcanized blend reveal two distinct phases for all four samples, as shown in **Fig. 1**. Due to the asymmetric polymer ratio (BR: NR=30:70), the BR (light phase) is seen to be dispersed in the NR matrix (dark phase). In a similar study by Jeon *et al.*[58], BR appeared dark phase and NR showed light in AFM phase images of NR/BR blend. This may be due to the scanning conditions as illustrated in detail by Wang and his coworkers' report[60].

© 2016. The authors – Published by Atlantis Press

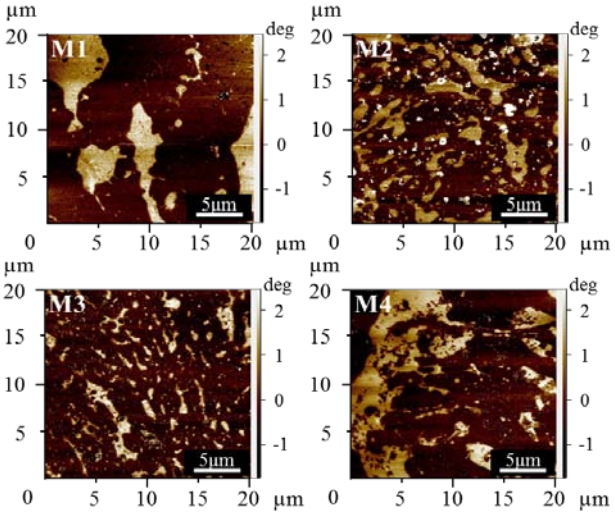

Figure 1. AFM phase images of NR/BR/LIR unvulcanized blend samples: M1, M2, M3 and M4.

It should be noted that from these results, the domain size of BR phases is generally large and the size distribution is broad in the uncompatibilized blends, as shown in Fig. 1M1. When a small amount of LIR was added to the NR/BR blend, the domain size of BR is decreased due to the compatibilization of LIR (Fig. 1M2). When LIR was mixed with NR first and then blended with BR, the BR phase is very uniformly dispersed and having the smallest domain size (Fig. 1M3). However, when LIR was first mixed with BR and then blended with NR, no obvious reduction in phase size of BR is observed (Fig. 1M4).

Since the interfacial tension is directly proportional to the domain size[61], we can conclude that the interfacial tension in M3 is the lowest in comparison with that of the other conditions. The reduction in BR phase size and interfacial tension in unvulcanized M3 blend might be attributed to the addition of LIR in the interface by this special mixing strategy. However, for M4, when LIR was first mixed with BR, LIR forms micelles with thick coronas, due to the asymmetric molecular weight ratio of butadiene to isoprene, cannot be breakup, and cannot migrate into the NR/BR interface, during the subsequent mixing with NR.

3.2 Rheological behaviors

Fig. 2 and Fig. 3 show the dynamic moduli and complex viscosities of unvulcanized and vulcanized NR/BR blend (M1) and NR/BR/LIR blends with three different mixing sequences (M2, M3, and M4). In the case of unvulcanized rubber blends (Fig. 2a), the addition of LIR causes the reduction of G′ especially for M3 at low frequency. Surprisingly, after vulcanization (Fig. 2b), only M4 vulcanizate has lower G′ than that of the control M1. Especially for M3, although the G′ at 0.01 Hz is only about one quarter of that for the control M1 before vulcanization, the G′ of the vulcanizate is 40% higher at whole frequency range than the control.

© 2016. The authors – Published by Atlantis Press

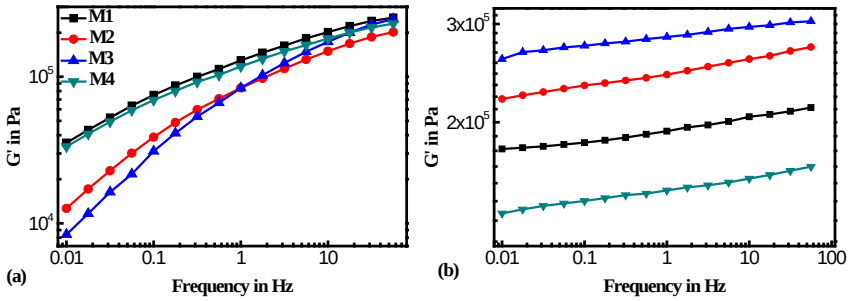

Figure 2. Dynamic storage moduli (G′) vs. frequency of unvulcanized (a) and vulcanized (b) NR/BR/LIR blends.

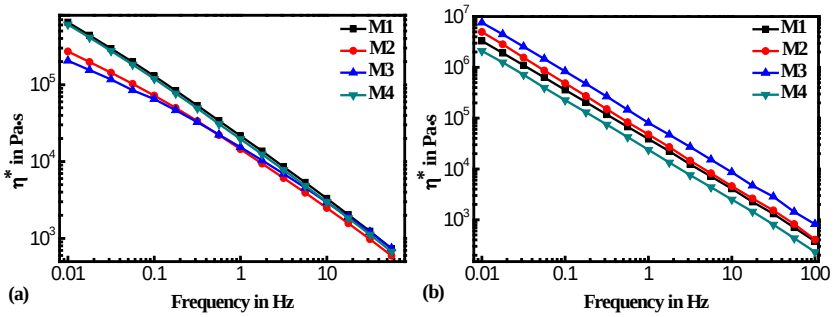

Figure 3. Complex viscosity (η*) vs. frequency of unvulcanized (a) and vulcanized (b) NR/BR/LIR blends.

These unusual results could be attributed to the "sliding effect" of short polyisoprene blocks of LIR before vulcanization, and the "networking effect" during vulcanization due to the reactive nature of the LIR at the interface of NR and BR (Fig. 4). Since the polyisoprene block of LIR copolymer has a molecular weight lower than the entanglement molecular weight M_e, which is 5097[62], under low frequency deformation, the isoprene block at the NR/BR interface can slide along, resulting in the low G′ before vulcanization. Since these LIR at the interface can co-vulcanize with the respective homopolymer component in NR/BR/LIR blend, these network will drastically reduce the mobility of these LIR molecules, and locking the two components NR and BR. Based on this proposed mechanism, the M3 should have the highest percentage of LIR molecules that reside at the interface of the binary blend.

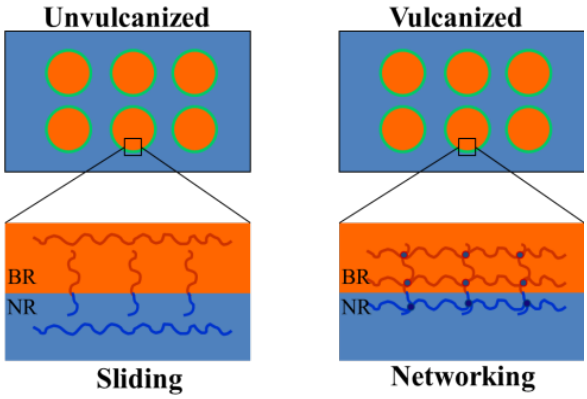

Figure 4. Schematic representation for the "sliding effect" and the "networking effect".

© 2016. The authors – Published by Atlantis Press

3.3 Mechanical properties

Table 2 shows the tensile properties of four different vulcanizates. The tensile strength and the elongation at break for M2 and M4 vulcanizates are comparable to that of the control M1 vulcanizate; while for M3 vulcanizate, both the of two values get significantly increased. This is consistent with the morphological results of AFM phase images (Fig. 1) and the rheological behaviors before and after vulcanization (Fig. 2 and Fig. 3) as described above, indicating that M3 has the most effective mixing sequence for the LIR compatibilization.

Table 2. Tensile properties of four different vulvanizates.

Compound	Elongation at break %	Tensile strength MPa
M1	607.5	6.2
M2	600.5	6.5
M3	648.3	7.5
M4	610.9	6.3

However, even the best possible compatibilization could only reduce the domain size of the blend without altering their miscibility. From Fig. 5, all the blends show the presence of two maxima corresponding to the glass transition temperature of NR and BR, although the peaks near -95 ^{o}C are not very clear. This indicates that the compatibilization does not promote molecular level miscibility.

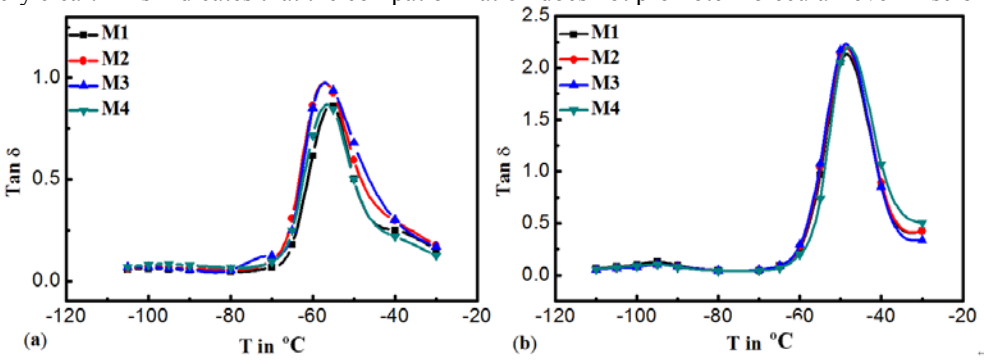

Figure 5. Tan δ vs. temperature for both unvulcanized and vulcanized blends at 10Hz.

In practice, an ideal material for high-performance tires should have a low tan δ value at 50-80 ^{o}C to reduce rolling resistance and save energy[63]. The smaller the tan δ value at 60 ^{o}C, the better is the rolling resistance of a tire. Fig. 6 shows the tan δ results of different rubber vulcanizates at -30-70 ^{o}C and 10 Hz. The tan δ values of M3 vulcanizate at 60 ^{o}C is the lowest, indicating the most improvement of rolling resistance.

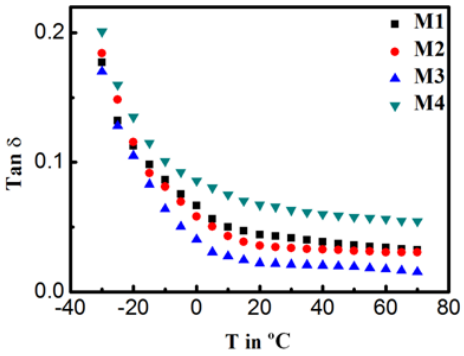

Figure 6. Temperature dependence of tan δ for different vulcanizates

© 2016. The authors – Published by Atlantis Press

3.4 Fatigue crack propagation behaviors

To characterize the safety and service life of final rubber products, an original real-time monitoring system of fatigue crack growth was employed. As shown in Fig. 7, the crack growth rate *dc/dn*[64], which is defined as the crack length increase per each cycle of deformation (nm/cycle), was measured at different loading conditions from the tear energy of 400 J/m^2 to1200 J/m^2.

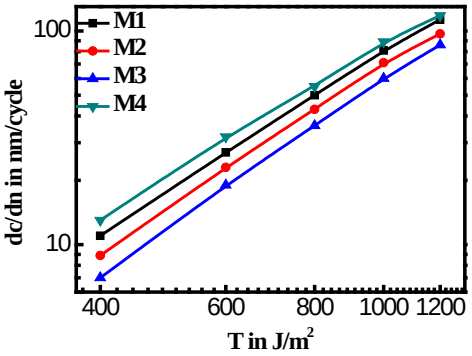

Figure 7. Crack growth rates of vulcanizates at different tear energy

Comparing with the control M1, the blend vulcanizate M2 has a slight decrease in *dc/dn* and thus some improvement of fatigue crack propagation resistance. The most significant reduction of *dc/dn* is achieved for M3 vulcanizate: at tear energy of 400 J/m^2, the *dc/dn* is reduced by half.

This improvement of crack resistance is consistent with the reduced domain size of the blends caused by LIR compatibilization. However, the vulcanized blend M4 has higher *dc/dn* values than the control M1 at all testing conditions. Although still consistent with the AFM morphology data, it is surprising that the addition of LIR would actually deteriorate its mechanical properties in the rubber system. As we suspected, in this case, LIR forms micelles in BR phase and never act as macromolecular surfactant when using this mixing sequence.

4 Conclusions

The remarkable effect of mixing sequence on the block copolymer compatibilization in a binary polymer blend is revealed. In this study, natural rubber (NR), high-cis butadiene rubber (BR) homopolymer, and a small amount of liquid butadiene-isoprene copolymer rubber (LIR), where the weight ratio of butadiene to isoprene is 90:10, were chosen to demonstrate the significant impact of this strategy of sequential mixing. Conclusions are drawn as follows:

(1) For the given component ratio of BR/NR=30:70, in addition to the NR/BR blend without LIR as the control (M1), three different mixing sequences were applied. In the conventional one-step mixing, NR, BR and LIR were mixed together at once (M2).

(2) Using sequential mixing, LIR was first mixed with one of the component, for example, NR, before mixing with BR, and we denote this as M3. If LIR was first mixed with BR, and then the mixture was blended with NR, we denote it as M4.

(3) The unvulcanized blend M3 has the finest dispersed BR phase and the lowest complex viscosity, and its vulcanizate has the best tensile properties (i.e. highest tensile strength and elongation at break) and the best rheological properties for tire applications (i.e. storage modulus, loss tangent at 60 ^{o}C, and lowest crack growth rate).

(4) The surprising improvement of both processing characteristics (such as complex viscosity) and mechanical properties (such as storage modulus) is explained by the “sliding effect” of the uncured sample, since the polyisoprene block of LIR copolymer has a molecular weight lower than the entanglement molecular weight M_e, and the “networking effect” after vulcanization, as the LIR at the interface can co-crosslink with the respective homopolymer component of the NR/BR/LIR blend.

© 2016. The authors – Published by Atlantis Press

(5) The M4 vulcanizate has the worst mechanical properties, and AFM image indicates the absence of the compatibilization effect, possibly due to the formation of micelles in BR phase.

Acknowledgements

The authors greatly acknowledge the financial support for this work provided by the Project of Natural Science Foundation of China (No. 21274070), the key scientific and technological innovation team of Zhejiang province (2011R50001), the Start-up funds of SUSTC (Y01216121).

References

1. Paul D R, Newman S. (Eds) "Polymer Blends", Academic Press, New York; (1978).
2. Utracki L A, Favis B D. *Handbook of Polymer Science and Technology, Marcel Dekker, Inc., New York*, 121-201(1989).
3. Folkes M J, Hope P S. (Eds) "Polymer Blends and Alloys", Chapman and Hall, London; (1993).
4. Nolley E, Barlow J W, Paul D R. *Polym. Eng. Sci.*, **20**, (5), 364-369 (1980).
5. Avgeropoulos G N, Weissert F C, et al. *Rubber Chem. Technol.* (1976, 49, (1), 93-104.
6. Shaw M T. *Polym. Eng. Sci.*, **22**, (2), 115-123(1982).
7. Sundararaj U, Macosko C W. *Macromolecules*, **28**, (8), 2647-2657(1995).
8. Epps T H, Chatterjee J, Bates F S. *Macromolecules,* **38**, (21), 8775-8784 (2005),.
9. Tureau M S, Rong L, Hsiao B S, et al. *Macromolecules*, **43**, (21), 9039-9048 (2010).
10. Haq E U, Toolan D T W, et al. *J Polym. Sci. Part B: Polym. Phys.* (2014), **52**, (15), 985-992.
11. Anastasiadis S H, Gancarz I, Koberstein J T. *Macromolecules*, **22**, (3), 1449-1453(1989).
12. Noolandi J, Hong K M. *Macromolecules*, **17**, (8), 1531-1537 (1984).
13. Noolandi J, Hong K M. *Macromolecules*, **15**, (2), 482-492(1982).
14. Noolandi J. *Polym. Eng. Sci.*, 24, (2), 70-78 (1984).
15. Vilgis T A, Noolandi J. *Macromolecules*, **23**, (11), 2941-2947(1990).
16. Leibler L. *Macromolecules* , **15**, (5), 1283-1290(1982).
17. Hu W, Koberstein J T, Lingelser J P, et al. *Macromolecules*, **28,** (15), 5209-5214 (1995).
18. Xu Y, Thurber C M, Macosko C W, et al. *Ind. Eng. Chem. Res.*, **53**, (12), 4718-4725 (2014).
19. Repollet-Pedrosa M H, Weber R L, Schmitt A L, et al. *Macromolecules*, **43**, (19), 7900-7902 (2010).
20. Albert J N L, Epps T H. *Mater. Today*, **13**, (6), 24-33 (2010).
21. Luo M, Epps T H. *Macromolecules*, **46**, (19), 7567-7579 (2013).
22. Widin J M, Kim M, Schmitt A K, et al. *Macromolecules* , 46, (11), 4472-4480(2013).
23. Wang Z G, Safran S A. *J. Phys. France.* 1990, **51**, (2), 185-200.
24. Adedeji A, Lyu S, Macosko C W. *Macromolecules*, **34**, (25), 8663-8668 (2001).
25. Kelley E G, Smart T P, Jackson A J, et al. *Soft matter* , **7,** (15), 7094-7102(2011).
26. Repollet-Pedrosa M H, Mahanthappa M K. *Soft Matter* , **9**, (32), 7684-7687(2013).
27. Schmitt A L, Repollet-Pedrosa M H, Mahanthappa M K. *ACS Macro Lett.* (2012, **1**, (2), 300-304.
28. Chen B, Li X L, Xu S Q, et al. *Polymer* , **43**, (3), 953-961(2002).
29. Macaúbas P H P, Demarquette N R. *Polymer* , **42,** (6), 2543-2554(2001).
30. Šmit I, Radonjič G, Hlavatá D. *Eur. polym. J.*, **40**, (7), 1433-1443 (2004).
31. Macosko C W, Guégan P, Khandpur A K, et al. *Macromolecules*, **29**, (17), 5590-5598 (1996).
32. Leibler L. In *Emulsifying effects of block copolymers in incompatible polymer blends*, Makromol. Chem. Macromol. Symp. pp 1-17 (1988).
33. Thomas S. *Polymer* , **33**, (20), 4260-4268(1992).
34. Riess V G, Kohler J, Tournut C, et al. *Makromol. Chem*, **101**, (1), 58-73 (1967).
35. Kohler J, Riess G, Banderet A. *Eur. polym. J.*, **4**, (1), 173-185 (1968).
36. Periard J, Riess G. *Colloid Polym. Sci.* , **253**, (5), 362-372(1975).
37. Lyatskaya Y, Gersappe D, Balazs A C. *Macromolecules* , **28**, (18), 6278-6283(1995).
38. Matos M, Favis B D, Lomellini P. *Polymer* , **36**, (20), 3899-3907(1995).

© 2016. The authors – Published by Atlantis Press

39. Harrats C, Fayt R, Jérôme R. *Polymer*, **43**, (3), 863-873 (2002).
40. Kim J, Gray M K, Zhou H, et al. *Macromolecules*, **38**, (4), 1037-1040 (2005).
41. Bell J R, Chang K, López-Barrón C R, et al. *Macromolecules*, 43, (11), 5024-5032 (2010).
42. Hermes H E, Higgins J S. *Polym. Eng. Sci.*, **38**, (5), 847-856 (1998).
43. Modesti M, Lorenzetti A, Bon D, et al. *Polymer* 46, (23), 10237-10245 (2005),.
44. Saleem M, Baker W E. *J. Appl. Polym. Sci.*, **39**, (3), 655-678(1990).
45. Xanthos M, Dagli S S. *Polym. Eng. Sci.*, **31**, (13), 929-935 (1991).
46. Sundararaj U, Macosko C W. *Macromolecules* , **28**, (8), 2647-2657(1995).
47. Chen Z R, Lanzarotta J M, Nagai Y, et al., U.S. Pat. 8,450,409 B2, (2013).
48. Lee M P, Moet A. *Rubber Chem. Technol*, **66**, (2), 304-316(1993).
49. Chen Z R., U.S. Pat. 12/870,260, (2011).
50. Kaang S, Jin Y W, Huh Y, et al. *Polym. Testing*, **25**, (3), 347-352 (2006).
51. Lake G J. *Prog. Rubber Technol*, **45**, 89-143 (1983).
52. Trent J S, Scheinbeim J I, Couchman P R. *Macromolecules* (1983), **16**, (4), 589-598.
53. Sain M M, Hudec I, Beniska J. *Polym. Testing*, **8**, (4), 249-259(1989).
54. Binnig G, Quate C F, Gerber C. *Phys. Rev. Lett.*, **56**, (9), 930(1986).
55. Sheiko S S, Möller M, Cantow H J, et al. *Polym. Bull.* , **31**, (6), 693-698(1993).
56. Tsukruk V V. *Rubber Chem. Technol.*, **70**, (3), 430-467 (1997).
57. Magonov S N, Whangbo M H. *VCH: New York* (1996).
58. Jeon I H, Kim H, Kim S G. *Rubber Chem. Technol.***76**, (1), 1-11 (2003).
59. Burnham N A, Colton R J, Pollock H M. *J. Vac. Sci. Technol. A*, **9**, (4), 2548-2556(1991).
60. Wang H, DjurišIć A B, Chan W K, et al. *Appl. Surf. Sci.* **252**, (4), 1092-1100(2005).
61. Wu S. *Polym. Eng. Sci.* **27**, (5), 335-343 (1987).
62. Fetters L, Lohse D, Richter D, et al. *Macromolecules*, **27**, (17), 4639-4647 (1994),.
63. Wang M J. *Rubber Chem. Technol*, **71**, (3), 520-589(1998).
64. Weng G, Yao H, Chang A, et al. *RSC Advances*, **4**, (83), 43942-43950 (2014).

© 2016. The authors – Published by Atlantis Press